2023 IEEE International Conference on Robotics and Automation (ICRA 2023)
May 29 - June 2, 2023. London, UK

Error-Domain Conservativity Control to Transparently Increase the Stability Range of Time-Discretized Controllers

Michael Rothammer[1] and Jee-Hwan Ryu[1]

***Abstract*— Time-discretization introduces an explicit time dependency for control laws that were originally designed to depend exclusively on an error variable: At different times, the control actions at the same error value might differ. Integrating the control action over the error reveals that this time dependency translates into the energy. It can directly cause active behavior when energy values at given error values decrease over time, potentially destabilizing the system. In this work, we aim to prevent energy values at given error values from decreasing over time. To this end, energies are recorded when error values are encountered for the first time. Linear interpolation of the recorded energy values provides a lower limit for energy as a function of the error value. This limit is enforced using an adaptive damping. The main contributions of this work include increasing the stability range with minimal amplitude control modifications, while promoting a symmetric behavior of control actions and energy. The approach's characteristics are shown in simulation and validated in experiments.**

***Index Terms*— Haptics, Adaptive Control**

I. INTRODUCTION

In recent years, haptics have become a key technology for human-machine interaction. One subcategory of haptics, kinesthetic feedback, involves rendering forces and torques for a human operator to feel. Haptic virtual environments have been shown to be an effective method of teaching motor skills for professionals [1], e.g. in the medical field [2]–[5], but is also applied in product development [6]–[8].

Many virtual environments are implemented in digital systems, implying a time-discretization of the control law. In the position-force relationship of a discretized virtual spring (see "unstabilized" trajectory in Fig. 1a), it can be observed that the pressing path differs from the releasing path. This directly indicates a *time-dependency* of the discretized spring force, whereas in the continuous domain, the force is only a function of the deflection for a spring. When integrating the force over the deflection to obtain energy, it becomes clear that also the virtual spring's deflection-energy relation becomes time-dependent, while the continuous case would be time-invariant. As a direct consequence of this time-dependency, the virtual spring releases more energy on the releasing path than it absorbed in the pressing path as can be seen in Fig. 1b. This behavior of releasing more energy than there has been absorbed is called *active*. In [9], it is explained how activity can cause instability and thereby significantly distort user experience.

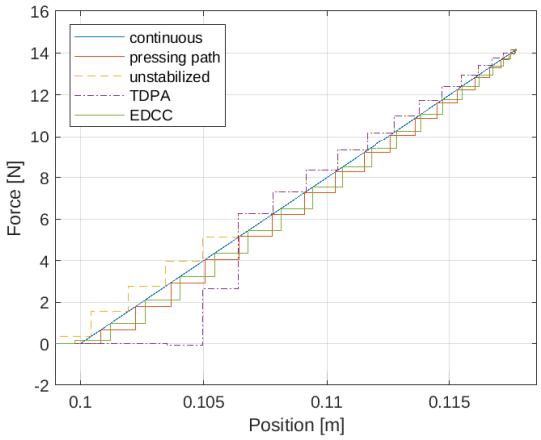

(a) Position-Force relation (all pressing paths are identical)

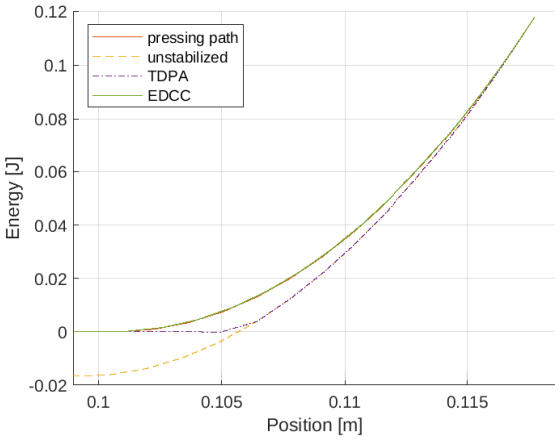

(b) Position-Energy relation (all pressing paths are identical)

Fig. 1: The behavior of EDCC as compared to TDPA. The trajectories coincide on the pressing path, but show significantly differing characteristics on the output path.

For that reason, although some other approaches have been investigated [10]–[12], the majority of stabilizing approaches in haptics are based on the concept of preventing active behavior of the haptic device, i.e. guaranteeing *passivity*.

The most prominent such passivation approach is the time-domain passivity approach (TDPA) [13], which consists of an energy observer that integrates the power flows into and out of the haptic interface, and modifies the control input using

This research was supported in part by Field-oriented Technology Development Project for Customs Administration through National Research Foundation of Korea(NRF) funded by the Ministry of Science & ICT and Korea Customs Service(2022M3I1A109507512), and in part by the Agency for Defense Development under Grant 21-CM-GU-04 funded by the Ministry of National Defense.

[1]The authors are with the Interactive Robotic Systems laboratory at the Korean Advanced Institute of Science and Technology. jhryu@kaist.ac.kr

an adaptive damping to ensure the device remains passive at all times. The passivation control input is minimal: It is only applied when explicitly required to avoid active behavior, and it is only applied in the minimum magnitude that suffices to passivate the device. However, as the passivation engages only when a negative energy value is predicted, active behavior can accumulate, so eventually a large amount of energy needs to be dissipated in few samples, requiring high-amplitude passivation control inputs.

In [14], the TDPA has been adjusted limit the energy to a reference value instead of a constant 0. This approach involves computing the desired energy level in a given system state to compare it with the true energy level. If the true energy level dropped below the limit, the adaptive damping dissipates the generated excess energy. An approximation approach for the desired energy levels of arbitrary controllers was briefly mentioned, but relies on a relatively inaccurate integration scheme that was not proven to be applicable to nonlinear virtual environments. Thus, in order to accurately realize this approach, explicit knowledge about the energy profile of the underlying controller is required.

The memory-based passivation approach (MBPA) [15] aims to avoid active behavior by enforcing an identical position-force relation for both pressing and releasing path. This is done by memorizing the force for every position on the pressing path. On the output path, the output force is read directly from memory instead of the underlying controller. For correct function, this requires specialized hardware that allows to instantly react to every encoder pulse to ensure that the position-force relation is not distorted by delay.

Recently, the deflection-domain passivity approach has been presented in [16]. Passivity is guaranteed on the deflection-domain for teleoperation with variable stiffness using a deflection-dependent limit for the stiffness value, simultaneously avoiding zero-stiffness phases.

Combining methods from [13]–[16], the error-domain conservativity controller (EDCC) contributes the following:

- Active energy generation of the controller is locally detected and inhibited, minimizing passivation input amplitude.
- It increases the stably renderable impedance range of haptic devices further than TDPA [13], which is widely acknowledged as a state-of the art stabilization approach.
- An even distribution of conservativity-ensuring control modifications promotes symmetry, as well as transparency with respect to the underlying controller.
- It does so without the need for any specialized hardware or explicit knowledge of the underlying controller.

This is achieved through *conservativity*, i.e. the energy levels at a given error value are ensured to not increase over time. This implies symmetry of the energy with regards to the error variable and also promotes symmetry of the control input. EDCC can ensure conservativity of any error-based controller.

This paper is structured as follows: Section II defines the proposed approach. Section III explains the most important properties of the approach using simulation results. Section IV shows the experimental validation of the approach, and Section V concludes the work.

II. Error-domain conservativity control

A. Conservativity observer

First, the energy of the system will be observed. The generalized control force $f[k]$ will be held constant between sampling operations. This means that the controller's stored energy $E[k]$ can be integrated *exactly* using [17]

$$E[k] = E[k-1] + f[k-1](x[k] - x[k-1]) = \sum_{i=1}^{k} f[i-1](x[i] - x[i-1]), \tag{1}$$

where $x[k]$ represents the generalized coordinate of the system, such that $\langle f, \dot{x} \rangle$ are power conjugates.

Many controllers, including many virtual environments and teleoperation approaches, compute the control input based on a so-called error or deflection

$$e[k] = x_\star[k] - x[k], \tag{2}$$

where $x_\star[k]$ usually denotes a desired equilibrium of $x[k]$. In virtual environments, $x_\star[k]$ can be the position of a virtual object's surface.

To ensure a time-invariant error-energy relation, the energy as a function of error will be memorized as a sparse map

$$E_{\text{mem}}[e[k]] = \begin{cases} E[k], & \text{if } \nexists\, E_{\text{mem}}[e[k]] \\ E_{\text{mem}}[e[k]], & \text{else} \end{cases}. \tag{3}$$

For every sample, it will be checked if the current error $e[k]$ has been visited before,

$$b_{\text{revisit}} \iff \exists\, e_{\text{lower}}, e_{\text{higher}} \text{ s. th. } e_{\text{lower}} \leq e[k] \leq e_{\text{higher}} \wedge \exists\, E_{\text{mem}}[e_{\text{lower}}], E_{\text{mem}}[e_{\text{higher}}]. \tag{4}$$

Whenever an error value is revisited (i.e. b_{revisit} is true (4)), we intend to find the energy previously associated with this error. However, since the energy memory will be populated only sparsely due to discretization, we will use the linear interpolation between stored error-energy pairs,

$$E_{\text{mem}}(e_{\text{revisit}}) = (e_{\text{revisit}} - e_{\text{low}}) \frac{(E_{\text{mem}}[e_{\text{high}}] - E_{\text{mem}}[e_{\text{low}}])}{(e_{\text{high}} - e_{\text{low}})} + E_{\text{mem}}[e_{\text{low}}], \tag{5}$$

with the nodes $e_{\text{high}} = \min(\{x \geq e_{\text{revisit}} | \exists\, E_{\text{mem}}[x]\})$ and $e_{\text{low}} = \max(\{x \leq e_{\text{revisit}} | \exists\, E_{\text{mem}}[x]\})$. Because the energy stored by the controller can be integrated as the physical work done by the piecewise constant generalized controller force along its generalized path (1), this interpolation is exact if $e_{\text{high}}, e_{\text{low}}$ exist and are not equal. This allows us to obtain the exact energy level at any previously experienced error.

When revisiting error values according to (4), we will check conservativity. In order to determine conservativity, we

compare the energy levels to those levels previously experienced at the given error, with the *dissipative conservativity condition* defined as

$$E[k] \geq E_{\text{mem}}(e_{\text{revisit}}[k]). \tag{6}$$

To achieve *strict conservativity*, it is possible to require

$$E[k] = E_{\text{mem}}(e_{\text{revisit}}[k]), \tag{7}$$

however, it is very common to use dissipative elements in control laws, which would be directly counteracted by satisfying this *strict conservativity condition*.

B. Conservativity controller

In order to avoid control actions that would compromise conservativity, a one step prediction assuming constant velocity as in [13] will be used to predict the conservativity parameters for the next sample time:

$$e_{\text{predicted}}[k] = e[k] + \dot{e}[k]\Delta t \tag{8a}$$

$$E_{\text{predicted}}[k] = E[k] + f_{\text{c}}[k]\dot{x}[k]\Delta t, \tag{8b}$$

where $f_{\text{c}}[k]$ is the underlying controller's control action.

Then, the predictive conservativity condition for the upcoming step is analogously to (6)

$$E_{\text{predicted}}[k] \geq E_{\text{mem}}(e_{\text{predicted}}[k]). \tag{9}$$

When (9) is violated, predicting a violation of (6), an adaptive damping force will be engaged to avoid the predicted conservativity violation,

$$f_{\text{d}}[k] = -\frac{(E_{\text{predicted}}[k] - E_{\text{mem}}(e_{\text{predicted}}[k]))}{\dot{x}[k]\Delta t}. \tag{10}$$

The resulting control action is $f[k] = f_{\text{c}}[k] + f_{\text{d}}[k]$.

If the constant velocity assumption holds, we can show

$$\begin{aligned} E[k+1] = E[k] + f[k]\dot{x}[k]\Delta t = \\ E[k] + f_{\text{c}}[k]\dot{x}[k]\Delta t - (E_{\text{predicted}}[k] - E_{\text{mem}}(e_{\text{predicted}}[k])) = \\ E_{\text{mem}}(e_{\text{predicted}}[k]) = E_{\text{mem}}(e[k+1]). \end{aligned} \tag{11}$$

This indicates that conservativity is enforced exactly. It should be noted that the constant velocity assumption will never be exactly satisfied. However, even if conservativity can not be achieved directly in one step, the energy difference $||E[k] - E_{\text{mem}}(e[k])||$ will decrease over time assuming a sufficiently small step size.

The initialization of the energy memory includes

$$E_{\text{mem}}[0] = 0. \tag{12}$$

This implies that the conservativity controller will ensure passivity at $e = 0$. For haptics, that means that a complete interaction including pressing and releasing path will be passive, as the energy on the virtual object's surface will be limited to zero. For the case of passive underlying controllers, passivity is ensured at all times.

It is also possible to explicitly ensure general passivity at all times by reformulating (6) to

$$E[k] \geq \max(E_{\text{mem}}(e_{\text{revisit}}[k]), 0), \tag{13}$$

and enforcing it regardless of (4). However, this implies that active controllers can not be applied transparently.

III. Simulations

The approach has been implemented in several simulations to show its most relevant characteristics in comparison with TDPA. A linear haptic interface with a mass of $0.1\,\text{kg}$ was simulated. The human operator was modeled as a constant force of $1\,\text{N}$. The control frequency was $1\,\text{kHz}$.

A. Stabilizing high virtual stiffnesses

For the first simulation, a virtual wall located at $x_\star = 0.1\,\text{m}$ with stiffness $18\,\text{kN}\,\text{m}^{-1}$ is considered.

In Fig. 2a, it can be seen that the virtual wall by itself releases twice as much energy in the releasing path as is absorbed in the pressing path. This behavior is called active and can lead to unstable behavior [18].

Fig. 2b shows how TDPA detects the active behavior and subsequently extracts energy from the system to passivate it. However, the passivation is engaged only once a negative energy value is predicted according to Eq. (8b). Because of the high amount of energy to be dissipated and resulting high passivation forces, the constant velocity assumption is violated, so TDPA can not fully avoid the predicted active behavior in one time step. The energy value becomes negative for one sample before the adaptive damping dissipates the remaining energy in a subsequent step.

In Fig. 2c, the energy never goes negative. That is because the excess energy created as a result of discretization violates the conservativity condition (6) even before it violates the passivity condition as defined in [13] for TDPA. Therefore, EDCC will start dissipating excess energy as soon as it is generated, instead of waiting for the energy prediction to go negative as TDPA does it. As a result, the releasing trajectory closely resembles the pressing trajectory with no apparent time-dependence of the error-energy relation.

For the simulation shown in Fig. 3, the stiffness was increased to $130\,\text{kN}\,\text{m}^{-1}$ and a damping of $0.09\,\text{N}\,\text{s}\,\text{m}^{-1}$ was added. It can be seen that without passivation (Fig. 3a), the contact is unstable. Also TDPA is unable to dissipate all the energy generated through the contact: Although it reduces the amplitude of unstable interactions, it fails to completely prevent them as shown in Fig. 3b. In Fig. 3c, it can be seen that the interaction quickly converges to a stable equilibrium when applying EDCC. It can be concluded that EDCC helps increase the stably renderable impedance range as a result of the more even distribution of the passivation input.

B. Symmetry

Fig. 1a shows a simulation with the same setup Section III-A at a reduced stiffness of $800\,\text{N}\,\text{m}^{-1}$ and without damping. It can be seen that in the pressing path, the position-force trajectory is a discretization of the ideal linear relation.

In the releasing path of the TDPA implementation, the trajectory is again a discretization of the linear relation in the first samples, however at differing values, revealing a time dependency of the position-force relation. This implies that the haptic device is active in this period, with the force on the releasing path exceeding the force on the pressing path at the same error value. Thus, energy is generated (see

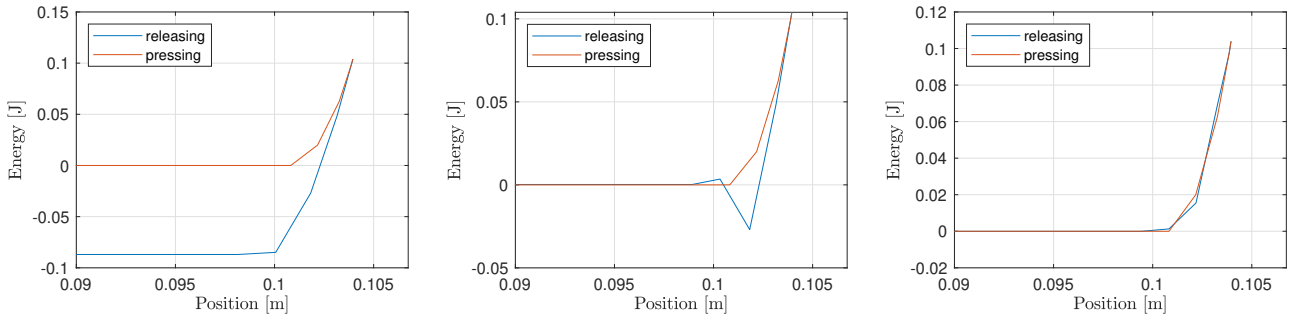

(a) No stabilization (b) TDPA (c) EDCC

Fig. 2: Comparison of position-energy trajectories at a stiffness of $18\,\mathrm{kN\,m^{-1}}$ with no damping.

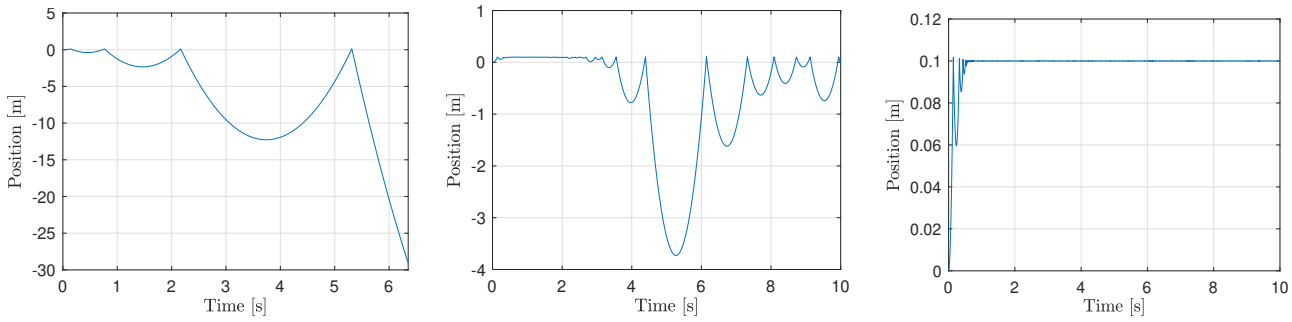

(a) No stabilization (b) TDPA (c) EDCC

Fig. 3: Comparison of position trajectories at a stiffness of $130\,\mathrm{kN\,m^{-1}}$ with a damping of $0.09\,\mathrm{N\,s\,m^{-1}}$.

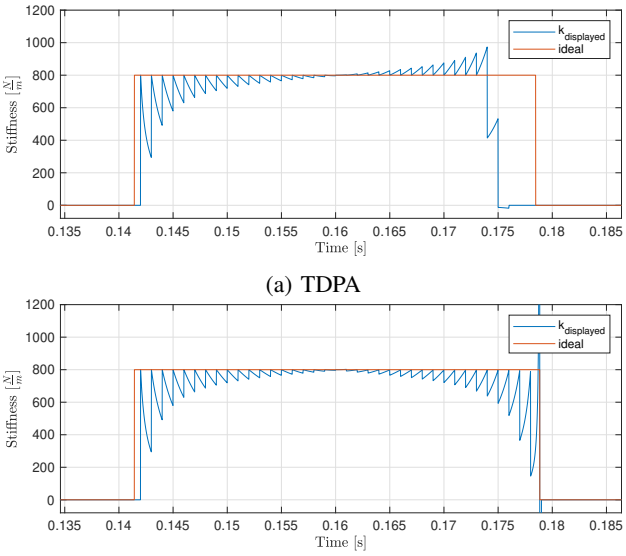

(a) TDPA

(b) EDCC

Fig. 4: Comparison of stiffness, computed as a ratio of discrete-time control forces and continuous-time positions.

Fig. 1b), causing TDPA's adaptive damping to engage at around $x = 0.107\,\mathrm{m}$, drastically reducing the subsequent forces in order to avoid overall active behavior. This results in a perceivable distortion of the haptic interaction as illustrated in the stiffness profile (Fig. 4a). Once TDPA modifies the forces, the displayed stiffness becomes virtually 0, compromising transparency.

Fig. 1a shows that the force on the releasing path exceeds the corresponding force on the pressing path for the first sample. However, it thereby directly violates the conservativity condition (6), so the adaptive damping force (10) is engaged. It reduces the subsequent force and the generated energy is dissipated already in the next sample. This process repeats throughout the entire releasing path, distributing the dissipation of the generated energy more evenly, and thus impacting the interaction forces less aggressively. In particular, the stiffness profile (Fig. 4b), shows that the behavior looks more *symmetric* as the releasing path is very similar to the pressing path.

C. Complex virtual environments

The proposed approach can ensure conservativeness of any error-based controller. It ensures that the controller remains conservative, i.e. the conservativity condition (6) is not violated.

To show the approach's broad applicability, we simulated nonlinear virtual environments with the control laws

$$e[k] = 0.1 - x[k] \tag{14a}$$

$$f_{c1}[k] = \begin{cases} 80000(e[k])^3, & \text{if } e[k] > 0 \\ 0, & \text{else} \end{cases} \tag{14b}$$

$$f_{c2}[k] = \begin{cases} 800e[k]\sin(200e[k]), & \text{if } e[k] > 0 \\ 0, & \text{else} \end{cases}. \tag{14c}$$

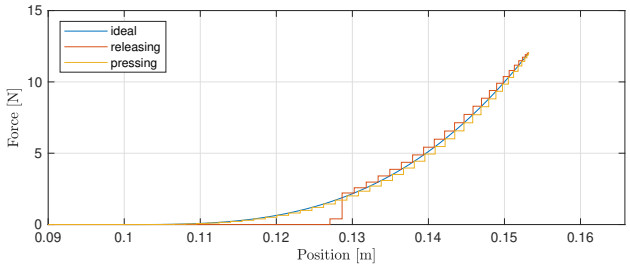

(a) TDPA

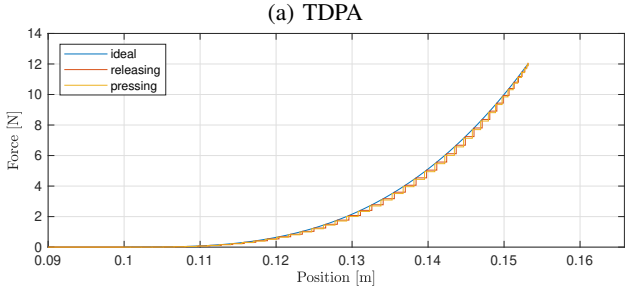

(b) EDCC

Fig. 5: Comparison of position-force trajectories.

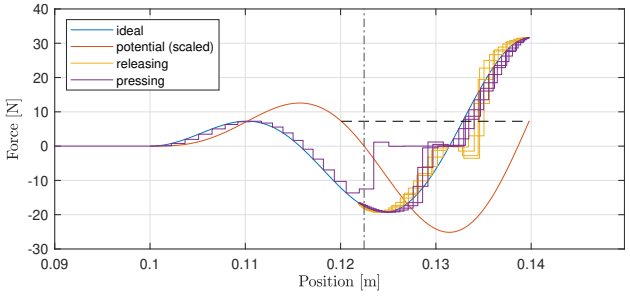

(a) TDPA

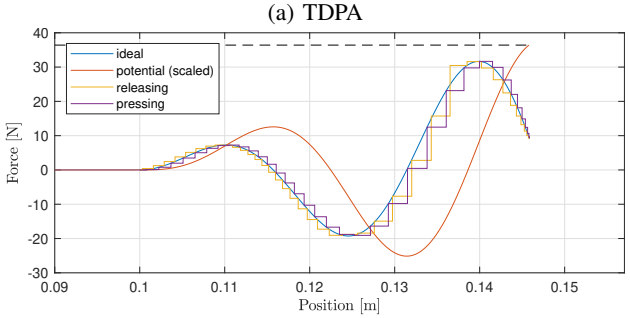

(b) EDCC

Fig. 6: Comparison of position-force trajectories.

The remaining simulation setup was identical to that in Section III-A.

For the control law (14b), Fig. 5 shows again a more symmetric force profile for EDCC as compared to TDPA, with TDPA reducing the force to almost zero for a large portion of the releasing path.

The control law (14c) represents the conservative force corresponding to a potential field that has minima with negative values, i.e. the global minimum is not located at $e[k] = 0$.

It can be seen in Fig. 6a that TDPA does not support this control law. Since the represented potential field has negative minima, the controller must become active to correctly display it. It should be noted that becoming active does not make the controller unstable in this case. However, it can be seen that when the potential crosses zero (dash-dotted line), TDPA engages immediately in the next sample, to counteract the active input of the underlying controller and maintain strict passivity. The adaptive damping is applied to extract energy from the system. It can be seen that the maximum penetration is reached at position $0.14\,\mathrm{m}$, which corresponds to a value of the virtual environment's potential field (dashed line) that is smaller than its local maximum at $0.115\,\mathrm{m}$, illustrating the energy dissipated by the adaptive damping. As a result, this maximum of the potential field can not be overcome in order to exit the virtual environment. The system continues cycling around the local minimum of the potential field.

Differently to TDPA, EDCC requires conservativity, but not strict passivity. As a result, it allows the controller to be active, so the control force can be displayed transparently even when the potential becomes negative without the adaptive damping engaging. Therefore, at the maximum penetration at $0.145\,\mathrm{m}$, the value of the potential field (dashed line) far exceeds the local maximum at $0.115\,\mathrm{m}$, indicating that the energy stored in the system is sufficient to overcome this maximum on the releasing path. Thus, the interaction with the locally active virtual environment can be completed in a fully transparent way with the interaction as a whole ensured to remain passive.

IV. Experiments

For the experimental evaluation, the haptic device from [15], with a single degree of freedom, driven by a brushed DC motor, was used. The motor was equipped with an encoder providing a resolution of 1024 pulses per revolution. A cable-based transmission increases the torque by a factor of 10 to drive a lever in an inverted pendulum configuration.

A. Validation of simulations

In [19], it has been shown that the human arm in the loop can greatly affect the behavior of haptic interfaces. To improve reproducibility of our results, we exploit the inverted pendulum structure of the haptic device and let gravity drive the interactions presented in this subsection. The haptic device's handle is released to drop into the virtual wall under its own weight, bouncing off the virtual wall.

A virtual wall with stiffness $50\,\mathrm{N\,m\,rad^{-1}}$ without damping was implemented as the virtual environment, with its surface at $x_\star = 0.5\,\mathrm{rad}$. We implemented both TDPA and EDCC. The virtual wall was designed intentionally soft to minimize the effects of limited encoder resolution and torque limits.

The error-energy behavior is illustrated by Fig. 7: The pressing and releasing path of the energy in Fig. 7a diverge over time, demonstrating significant time dependency, whereas the releasing path in Fig. 7b almost exactly follows

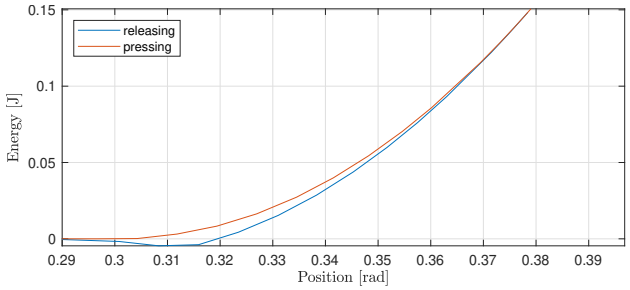

(a) TDPA

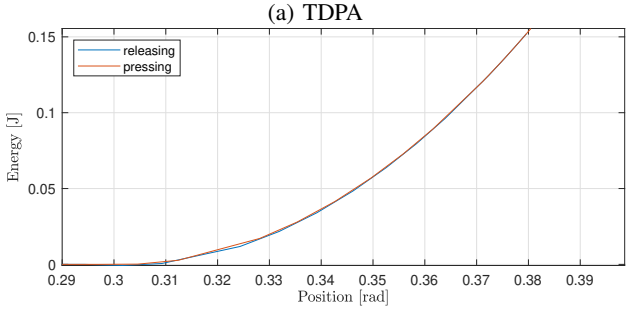

(b) EDCC

Fig. 7: Comparison of position-energy trajectories.

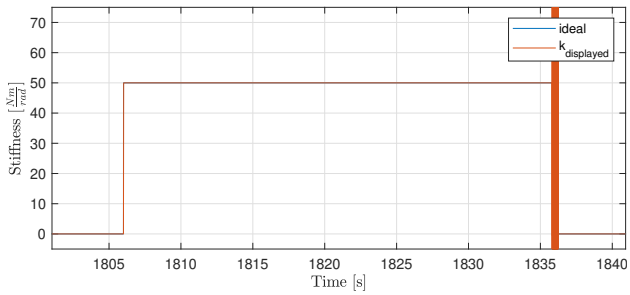

(a) TDPA

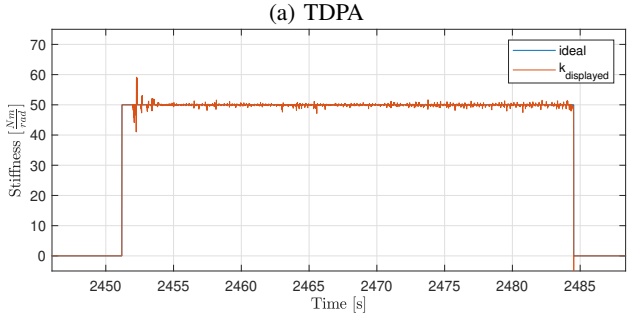

(b) EDCC

Fig. 9: Comparison of stiffness profiles over prolonged time.

the pressing path. These experiments confirm the simulation results.

B. Prolonged interaction

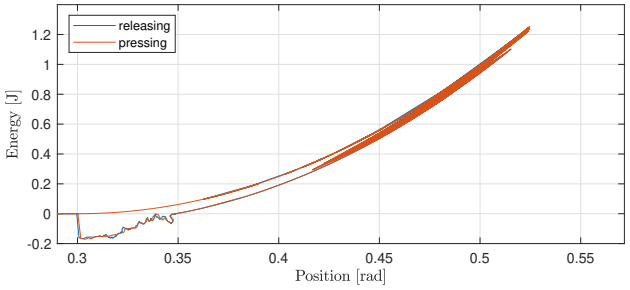

(a) TDPA

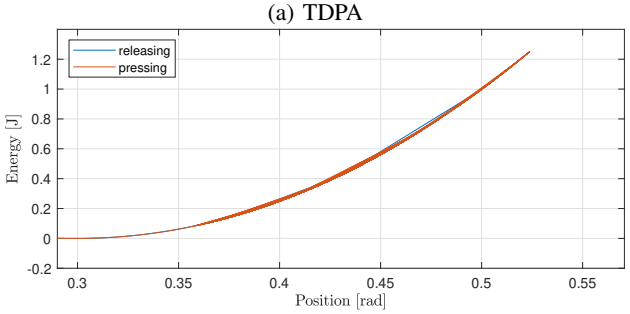

(b) EDCC

Fig. 8: Comparison of position-energy trajectories.

Virtual springs will continue generating energy through the entire time they are interacted with. Thus, for prolonged interactions, relatively large quantities of active energy can accumulate when applying TDPA. This phenomenon has been experimentally reproduced by manually interacting with the virtual environment for 30 s. The energy drift can be seen clearly in Fig. 8a. When the contact is eventually terminated, TDPA's energy observer detects the accumulated activity and the passivity controller causes considerable modifications of the control input, compromising transparency, as can be seen in the stiffness profile (Fig. 9a). EDCC however uses minor modifications distributed over the entire time of the interaction. Thereby energy buildup can be avoided (see Fig. 8b). This manifests in a more consistent stiffness profile as shown Fig. 9b.

V. Conclusion

In this paper, a novel memory-based conservativity-ensuring approach has been presented. By ensuring a time-invariant relation between error and energy, it can increase the stably renderable impedance range of haptic interfaces. In addition, the stabilization input is more evenly distributed and of smaller amplitude than that of TDPA, thus providing symmetry and increasing transparency.

EDCC was formulated for one-dimensional systems. Although for many applications it can be applied on the amplitude $\|\vec{e}\|$ of multidimensional error variables $\vec{e}$, a more general solution would be desirable, making it a subject of future work.

Furthermore, EDCC has been shown in this work applied to haptics. However, it is applicable to a wide range of different controllers whose conservativeness is desired. Future work will include an investigation of the applicability to teleoperation and motion control.

REFERENCES

[1] D. Feygin, M. Keehner, and R. Tendick, "Haptic guidance: experimental evaluation of a haptic training method for a perceptual motor skill," in *Proceedings 10th Symposium on Haptic Interfaces for Virtual Environment and Teleoperator Systems. HAPTICS 2002*, 2002, pp. 40–47.

[2] Y. Shi, Y. Xiong, X. Hua, K. Tan, and X. Pan, "Key techniques of haptic related computation in virtual liver surgery," in *2015 8th International Conference on Biomedical Engineering and Informatics (BMEI)*, 2015, pp. 355–359.

[3] X. Shen, A. Hamam, F. Malric, S. Nourian, N. R. El-Far, and N. D. Georganas, "Immersive haptic eye tele-surgery training simulation," in *2007 3DTV Conference*, 2007, pp. 1–4.

[4] B. Pérez-Gutiérrez, D. M. Martinez, and O. E. Rojas, "Endoscopic endonasal haptic surgery simulator prototype: A rigid endoscope model," in *2010 IEEE Virtual Reality Conference (VR)*, 2010, pp. 297–298.

[5] J. Madera, C. Peters, and A. M. Fey, "A novel pulley-based simulator for ureteroscopy with visuo-haptic feedback," in *2022 IEEE Haptics Symposium (HAPTICS)*, 2022, pp. 1–6.

[6] S. Shin, I. Lee, H. Lee, G. Han, K. Hong, S. Yim, J. Lee, Y. Park, B. K. Kang, D. H. Ryoo, D. W. Kim, S. Choi, and W. K. Chung, "Haptic simulation of refrigerator door," in *2012 IEEE Haptics Symposium (HAPTICS)*, 2012, pp. 147–154.

[7] M. Bordegoni, F. Ferrise, and J. Lizaranzu, "Use of interactive virtual prototypes to define product design specifications: A pilot study on consumer products," in *2011 IEEE International Symposium on VR Innovation*, 2011, pp. 11–18.

[8] W. Zhu and Y.-S. Lee, "Five-axis pencil-cut planning and virtual prototyping with 5-dof haptic interface," *Computer-Aided Design*, vol. 36, no. 13, pp. 1295–1307, 2004.

[9] J. E. Colgate, M. C. Stanley, and J. M. Brown, "Issues in the haptic display of tool use," in *Proceedings 1995 IEEE/RSJ International Conference on Intelligent Robots and Systems. Human Robot Interaction and Cooperative Robots*, vol. 3. IEEE, 1995, pp. 140–145.

[10] P. G. Griffiths and R. B. Gillespie, "Recovering haptic performance by relaxing passivity requirements," in *World Haptics 2009 - Third Joint EuroHaptics conference and Symposium on Haptic Interfaces for Virtual Environment and Teleoperator Systems*, 2009, pp. 326–331.

[11] J. Gil, A. Avello, A. Rubio, and J. Florez, "Stability analysis of a 1 dof haptic interface using the routh-hurwitz criterion," *IEEE Transactions on Control Systems Technology*, vol. 12, no. 4, pp. 583–588, 2004.

[12] M. Minsky, O.-y. Ming, O. Steele, F. P. Brooks Jr, and M. Behensky, "Feeling and seeing: issues in force display," in *Proceedings of the 1990 symposium on Interactive 3D graphics*, 1990, pp. 235–241.

[13] B. Hannaford and J.-H. Ryu, "Time-domain passivity control of haptic interfaces," *IEEE transactions on Robotics and Automation*, vol. 18, no. 1, pp. 1–10, 2002.

[14] J.-H. Ryu, B. Hannaford, C. Preusche, and G. Hirzinger, "Time domain passivity control with reference energy behavior," in *Proceedings 2003 IEEE/RSJ International Conference on Intelligent Robots and Systems (IROS 2003)(Cat. No. 03CH37453)*, vol. 3. IEEE, 2003, pp. 2932–2937.

[15] T. H. Do and J.-H. Ryu, "Memory based passivation method for stable haptic interaction," in *2011 IEEE World Haptics Conference*. IEEE, 2011, pp. 409–414.

[16] M. Panzirsch, M. Sierotowicz, R. Prakash, H. Singh, and C. Ott, "Deflection-domain passivity control of variable stiffnesses based on potential energy reference," *IEEE Robotics and Automation Letters*, vol. 7, no. 2, pp. 4440–4447, 2022.

[17] J.-H. Ryu, Y. S. Kim, and B. Hannaford, "Sampled-and continuous-time passivity and stability of virtual environments," *IEEE Transactions on Robotics*, vol. 20, no. 4, pp. 772–776, 2004.

[18] J. Colgate and G. Schenkel, "Passivity of a class of sampled-data systems: application to haptic interfaces," in *Proceedings of 1994 American Control Conference - ACC '94*, vol. 3, 1994, pp. 3236–3240 vol.3.

[19] H. S. Woo and D. Y. Lee, "Passivity analysis of a 1-dof haptic system with consideration of human arm impedance," in *2008 International Conference on Control, Automation and Systems*, 2008, pp. 1296–1300.